Title
LARGE CONTRIBUTION OF DEEP INELASTIC PROCESSES TO REACTIONS OF 40Ar AND 48Ca WITH 238U

Author
Otto, R.J.

Publication Date
1978-02-01

Submitted to Zeitschrift für Physik A

LBL-7188
Preprint c.2

LARGE CONTRIBUTION OF DEEP INELASTIC PROCESSES TO REACTIONS OF ^{40}Ar AND ^{48}Ca WITH ^{238}U

R. J. Otto, D. J. Morrissey,
G. T. Seaborg, and W. D. Loveland

February 6, 1978

Prepared for the U. S. Department of Energy
under Contract W-7405-ENG-48

LARGE CONTRIBUTION OF DEEP INELASTIC PROCESSES TO REACTIONS OF ^{40}Ar AND ^{48}Ca WITH ^{238}U

R. J. Otto, D. J. Morrissey, G. T. Seaborg
Lawrence Berkeley Laboratory
and
Department of Chemistry
University of California
Berkeley, California 94720

W. D. Loveland
Oregon State University
Corvallis, Oregon 97331

Abstract

Differential recoil range distributions have been measured for heavy-reaction products ranging from Te(Z = 52) to quasielastic transfer products near the charge and mass of the targets for the reactions of 276 MeV $^{48}Ca + ^{238}U$, 237 MeV and 250 MeV $^{40}Ar + ^{238}U$, and 259 MeV $^{40}Ar + ^{197}Au$. The measured recoil range distributions for the $^{40}Ar + ^{197}Au$ reaction agree with range distributions calculated from the known projectile-like fragment angular distributions for this reaction. The angular distributions of recoil products formed in the uranium target reactions are deduced and show that the products in the $_{75}Re$ to $_{83}Bi$ region have backward peaked angular distributions characteristic of deep inelastic reactions. The heavy product angular distributions smoothly vary from a $(1/\sin\theta)$ shape to an exponential shaped backward peak as the atomic number of the product increases from 52 to 83. The trend in the deduced angular distributions for those elements for which recoil range distributions were

determined in the ^{40}Ar + ^{197}Au reaction and the 250 MeV ^{40}Ar + ^{238}U reaction is similar, suggesting that just as for the Ar + Au system the composite system for the uranium target reaction is also not fully equilibrated along the mass asymmetry coordinate. These conclusions show that the fraction of the total reaction cross section resulting in complete fusion must be re-evaluated for the ^{40}Ar + ^{238}U reaction and similar heavy-target reactions.

I. Introduction

Nuclear shell effects have played an important role in many aspects of the fission process. Thus we noted with great interest the recent report [1] that a superheavy nucleus may undergo very asymmetric fission due to nuclear shell effects. Kalpakchieva et al. [1] have interpreted the results of correlated fragment mass distribution measurements for the ^{40}Ar + ^{243}Am reaction as possible evidence for the existence of highly mass asymmetric fission of the compound nucleus $^{283}[113]$; also, they have attributed the observed asymmetry ($A_H/A_L \approx 2.5$) to the preferential formation of a heavy fragment near the doubly magic ^{208}Pb region. Such behavior has been predicted on theoretical grounds by Sandulescu and Greiner [2]. However, it has been shown in studies of ^{40}Ar ions with gold and silver targets [3-8] that it is difficult to distinguish between products arising from deep inelastic transfer reactions and those products arising from complete fusion processes on the basis of fragment mass and energy distributions alone. Therefore, as a further test of the correctness of the inferences of Kalpakchieva et al. [1] and because of general interest in the extent of complete fusion processes in the reaction of ^{40}Ar and ^{48}Ca projectiles with heavy targets, we have deduced angular distributions from differential recoil range distributions of heavy products from the reaction of these projectiles with uranium targets. Based upon these angular distributions we report the existence of a large contribution of non-complete fusion processes leading to products in the ^{208}Pb region, that are part of a broad symmetric mass distribution centered at approximately one-half the mass of the composite system, in the case of $^{40}Ar + ^{238}U$ [9]. This result casts some doubt on the validity of the conclusions of Kalpakchieva et al. [1] and creates a need to re-evaluate the previously inferred magnitudes of the complete fusion process in these reactions [9,10].

It is generally accepted [11,12] that heavy-ion reactions that reach the stage of complete fusion will have fission product center-of-mass angular distributions that are symmetric about 90° and approach $1/\sin\theta$. The observation of products having angular distributions with this symmetry property is a necessary, although not a sufficient criterion for identification of a complete fusion-fission product. Therefore, the observation of forward peaking in excess of $1/\sin\theta$ and its dependence upon the Z difference between the actual fragment and the projectile are crucial in ruling out complete fusion processes [11].

In our tests of the conclusions of Kalpakchieva et al. [1] we have deduced the angular distribution of heavy products in the lead region from the reaction of 276 MeV $^{48}Ca + ^{238}U$, 237 MeV and 250 MeV $^{40}Ar + ^{238}U$ using a recoil distribution technique. Otto et al. [13] have shown that the differential recoil range distribution of target-like products $(72 \leq Z \leq 84)$ from the reaction of krypton and xenon ions with gold targets and krypton ions with uranium targets can be directly correlated with measured side peaked angular distributions of the complementary projectile-like fragments. Furthermore, we have measured recoil range distributions for products ranging from Te(Z = 52) to Au(Z = 79) produced in the reaction of 259 MeV $^{40}Ar + ^{197}Au$ and correlated these range distributions with the measured angular distributions [4,7] for the complementary light fragments formed in deep inelastic reaction with the same target and projectile.

II. Experimental

Table I summarizes the reactions studied and compares the excitation energies assuming compound nucleus formation. In all of the reactions listed in Table I the fission barrier [15] for the highly rotating compound nucleus is expected to be zero. A detailed description of the experimental recoil range distribution method has been given [13], and will only be briefly covered in this report. Thin UF_4 targets of thickness $\sim$0.7 mg/cm^2 supported on a 3.4 mg/cm^2 aluminum backing, or a 2.4 mg/cm^2 gold foil target, were placed directly in front of a stack of 1.1 mg/cm^2 Al recoil foils and irradiated as a single package. Following the irradiation the target and Al recoil foils were separated, taped to aluminum planchets and assayed by x-ray spectrometry. X-ray spectra were obtained for the energy region between 10 and 100 keV. The resolution of the spectrometer system was 650 eV FWHM. Additional recoil foils were also placed in front of the target foil whenever there was a possibility of fragment emission into the backward hemisphere in the laboratory, so that in all cases essentially 100% of the reaction products would have been stopped in one or another of the recoil foils. The atomic numbers of the reaction products could then be assigned, based on the energies of their corresponding x-ray peaks observed in the spectra. The differential recoil range distribution for a given element or set of elements was obtained from the relative count rate of the observed x rays in each of the recoil foils. Average growth and decay corrections were made for each element identified by following the growth and decay of the observed x rays in one of the recoil foils. We report here the results for selected representative elements from the x-ray spectra obtained for the systems studied.

III. Results and Discussion

The experimental recoil range distributions shown in Figs. 1-3 can be understood as follows. There is one range distribution derived for each selected x-ray peak or group of x-ray peaks identified in the x-ray spectra. The ordinate labeled "Percent (Recoil Product Activity) Per Recoil Foil" represents the relative number of atoms, in each recoil foil, of the identified element. The range distribution plots are shown in a histogram fashion because of the integral nature of the recoil foils. A way to visualize the relationship between the axial recoil range distribution and the center-of-mass angular distribution, $(d\sigma/d\theta)$, is to imagine that the probabilities of finding a given product (stopped at the end of its range) in the three-dimensional coordinate space around the target are projected onto a line defined by the beam axis. These probabilities summed into bins equivalent to the thickness of the recoil foils give the differential axial recoil range distribution for that product.

To correlate the measured recoil range distributions with the center-of-mass angular distribution of a given reaction product, we have written a code [13] that calculates the recoil range distribution for any given experimental conditions and for any chosen center-of-mass angular distribution. The code uses a two-step reaction model. The fundamental assumptions in this model are: 1) the target and projectile form a composite system by sticking together for some period of time that may be long (complete fusion) or short (deep inelastic scattering) when compared with the rotational period of the system. 2) The merged or amalgamated system separates into two fragments with a total kinetic energy determined by the Coulomb repulsion of two touching spheres and this fission kinetic energy is independent of the angle of emission. This second assumption is supported by many ^{40}Ar ion studies [3-8] and is applicable to deep inelastic as well as complete fusion reactions. The final calculation of the recoil range distribution code translates the calculated laboratory fragment energies at every 0.1° in the laboratory into ranges in Al using a parametrization [13] of the Northcliffe-Schilling tables [16].

Figure 1 shows a comparison of the measured (solid lines) and calculated (dashed lines) recoil range distributions for products ranging in atomic number from $Z = 52$ to $Z = 79$ and formed in the reaction of 259 MeV $^{40}Ar + ^{197}Au$. The angular distribution used to predict the recoil range distribution for $_{79}Au(_{80}Hg)$ products is a Gaussian peaked at the classical grazing angle and has a FWHM of 30°. This angular distribution was chosen since these products are expected to be quasielastic transfer products. The angular distributions used to calculate recoil range distributions for the $_{74}W(_{75}Re)$ and $_{69}Tm$ products correspond in shape (180° reversed) to the previously measured angular distributions for the complementary light argon-like fragments

[4,7] from the reaction of $^{40}Ar + ^{197}Au$. In this case the argon-like fragment angular distributions are forward peaked so that the complementary heavy gold-like fragments must be backward peaked in the c.m. system. The angular distribution for $_{67}Ho$, $_{58}Ce$ and $_{52}Te$ was taken to be $1/(\sin\theta + 0.1)$. (An arbitrary constant of 0.1 was added to $\sin\theta$ to provide more realistic angular distributions by preventing the distributions from becoming infinite at 0° and 180°.) The Northcliffe-Schilling ranges somewhat overestimate the maximum ranges of the fragments [17] and predict that a few percent of the activity would be found beyond the longest and shortest ranges actually observed. It is clear from Fig. 1 that the shape of the recoil range distributions sensitively reflect trends in the angular distributions as a function of the Z of the product. A comparison of the $_{74}W(_{75}Re)$ recoil range distribution with the $_{67}Ho$, $_{58}Ce$ or $_{52}Te$ recoil range distribution shows the types of shapes expected for backward peaked and $1/\sin\theta$ angular distributions, respectively.

Figure 2 shows recoil range distributions of the product ^{237}Pu (detected via its 59.7 keV gamma ray), and a composite recoil range distribution of Te, I, Xe and Cs species and Hf, Ta, W, Re and Os species from the combined count rate of x rays having energies between 27.5 keV to 31.0 keV and 55.9 keV to 62.0 keV, respectively. These results were taken from spectra obtained from the 250 MeV $^{40}Ar + ^{238}U$ reaction. Since ^{237}Pu is expected to be primarily a quasielastic transfer product, a Gaussian shaped angular distribution peaked at the classical grazing angle with a FWHM of 30° was used to calculate the theoretical recoil range distribution shown as a dashed line. The experimental recoil range distribution (solid line) from the combined x rays from Te, I, Xe and Cs products is compared with the calculated recoil range distribution (dotted line) for a $1/\sin\theta$ angular distribution [actually $1/(\sin\theta + 0.1)$]. The half-life analysis and relative intensities of the x rays indicate that ^{126}I which is known to be part of the broad symmetric fusion-fission mass distribution for this reaction [9,18] was the prominent fragment in the Te to Cs region. Again the calculated recoil range distributions predict somewhat longer ranges than observed; however, the relative shapes are in good agreement. The experimental recoil range distribution for products between Hf and Os (solid line) is in good agreement with the calculated recoil range distribution (dashed line) derived from an exponentially decreasing backward peaked angular distribution.

Fig. 3(A) shows the experimental recoil range distributions for the Hg(Tl) products corresponding to the x-ray peak that is a superposition of the $K\alpha_1$ x ray of Hg and the $K\alpha_2$ x ray of Tl. As shown in Fig. 3(A), these similar results come from the two reactions ^{48}Ca + ^{238}U and ^{40}Ar + ^{238}U and correspond to three different excitation energies. Calculated recoil range distributions for the Hg(Tl) products from these three reactions are shown in Fig. 3(B), and are based on three different assumptions about the heavy product angular distribution. These three functional forms are shown in Fig. 3(C). The Hg(Tl) recoil data correspond most closely to the predictions of the simple backward peaked angular distributions (corresponding to a forward peaked projectile-like fragment distribution); however, there is a small discrepancy at the longer ranges indicating the possibility of a small (1/sinθ) contribution. To test such an effect we have used a backward peaked angular distribution mixed with a 10% (1/sinθ) contribution (actually 1/sinθ + 0.01). The experimental results, shown in Fig. 3(A), fall between the calculated distributions, (shown in Fig. 3(B)), expected for a backward peaked plus 1/sinθ angular distribution (dotted line) and the simple backward peaked angular distribution represented by an exponential decreasing function (solid line).

Measurements of the product mass distributions [19] for the reaction of 288 MeV ^{40}Ar with a thick ^{197}Au target ($\bar{E} \approx 210$ MeV) as well as in beam counter studies [4,7] for the same reaction at somewhat different energies show that after eliminating the quasielastic transfer distribution, the remaining products form a broad symmetric mass distribution peaked at approximately one-half the mass of the composite system. However, the angular distributions [4,7] show a transition from forward peaking, for the light projectile-like fragment, to a (1/sinθ) angular distribution as the mass and charge of the two fragments approach symmetry. This trend is also observed for the heavier products both in our recoil range experiments and by Lucas et al. [8]. Such a trend can be explained in terms of a dynamical diffusion process occurring within the composite $^{40}Ar + ^{197}Au$ system. The longer the projectile and target nuclei remain in contact, the more mass exchange takes place (leading to a more symmetric mass division) and the greater the "memory loss" of the composite system, leading to final products having a (1/sinθ) angular distribution. Such a dynamical diffusion process has been used to explain the deep inelastic transfer reactions [11]. In fact, as far as these data are concerned, the deep inelastic mechanism could be operative over the entire mass region for a projectile even as light as ^{40}Ar and it would not be necessary to invoke the fusion-fission mechanism to account for the products corresponding to symmetric division of the composite system. An alternative approach [4,8] is to analyze the mass and angular distributions in terms of a superposition of two components: a fission component corresponding to relatively symmetric masses having (1/sinθ) type angular distributions, and a deep inelastic component with an associated Gaussian shaped mass distribution peaked near the target (and projectile) masses having products with a backward peaked (and forward peaked) angular distributions.

Kratz et al. [9] have shown that the products from $Z = 50$ to $Z = 83$ in the reaction of $\leq$288 MeV $^{40}Ar + ^{238}U$ ($\bar{E}_{lab} \sim 241$ MeV) are part of a broad symmetric mass distribution centered at approximately $Z = 58$. The recoil range distributions for products from $Z = 52$ to $Z = 94$ from the reaction of 250 MeV $^{40}Ar + ^{238}U$ shown in Fig. 2 indicate that there is a transition from backward peaked angular distributions to angular distributions approaching $1/\sin\theta$ as a function of decreasing mass asymmetry of the two fragments from the breakup of the composite system. This transition is similar to the one observed in the Ar + Au reaction [4-8]. Furthermore, Fig. 3 shows that all of the Hg(Tl) product angular distributions remain backward peaked as the bombarding energy is decreased. The interpretation of this angular distribution trend would appear to be the same as the interpretation given for the $^{40}Ar + ^{197}Au$ reaction. The observed lead-like products are clearly the result of the deep inelastic transfer reaction process. The backward peaked angular distribution of the Hg(Tl) products indicates that the composite system has not reached a state of complete fusion before breaking into two fragments with one fragment in the doubly magic lead region. The same conclusion can be drawn even for more symmetric division of the composite system.

Since we have observed predominantly backward peaked angular distributions for $Z = 72$ products (separated by as much as 20 Z units from the target), it would be necessary to invoke a very unusual deep inelastic component mass distribution to explain simultaneously the product mass and angular distributions in terms of a "two-component" model of the reaction.

IV. Conclusions

We believe that our data indicate that non-complete fusion (and non-compound nuclear) processes account for a large portion of the mass distribution of the ^{48}Ca + ^{238}U reaction; and, of the broad symmetric mass distribution of the ^{40}Ar + ^{238}U reaction [9] previously attributed to "fusion-fission." It would appear to us that earlier work [9,10] on the ^{40}Ar + ^{238}U system may have overestimated the cross section due to complete fusion processes. Furthermore, since we see little difference between the compound nuclei expected to be produced in this study and the work of Kalpakchieva et al. [1], we might expect that a careful study of the angular distribution trends as a function of Z for fragments in the Pb region would reveal backward peaked angular distributions for the ^{40}Ar + ^{243}Am reaction. Such an observation would rule out a complete fusion-fission process leading to the observed mass distribution asymmetry. Perhaps the results of Kalpakchieva et al. could be taken as strong evidence for shell stabilization effects in the deep inelastic process.

Acknowledgments

The authors would like to thank Hermann Grunder and the SuperHILAC crew as well as B. Gavin and co-workers for providing the ^{40}Ar + ^{48}Ca beams for these experiments. This work was supported in part by the High Energy and Nuclear Physics Division of the Department of Energy.

References

1. Kalpakchieva, R., Oganessian, Yu. Ts., Penionzhkevich, Tu. E., Sodan, H.: Z. Physik A283, 253 (1977).

2. Sandulescu, A., Greiner, W.: J. Phys. G3, L189 (1977).

3. Galin, J., Moretto, L. G., Babinet, R., Schmitt, R., Jared, R., Thompson, S. G.: Nucl. Phys. A255, 472 (1975).

4. Ngo, C., Peter, J., Tamain, B., Berlanger, M., Hanappe, F.: Z. Physik A283, 161 (1977).

5. Artukh, A. G., Gierlik, E., Gerstenberger, R., Gridnev, G. F., Mezentsev, A. N., Miheev, V. L., Salamatina, T. S., Volkov, V. V., Zlokazov, V. B.: JINR Report E7-10464.

6. Galin, J., Gatty, B., Guerreau, D., Lefort, M., Tarrago, X., Agarwal, S., Babinet, R., Gauvin, B., Girard, J., Nifenecker, H.: Z. Physik A283, 173 (1977).

7. Moretto, L. G., Galin, J., Babinet, R., Fraenkel, Z., Schmitt, R., Jared, R., Thompson, S. G.: Nucl. Phys. A259, 173 (1976).

8. Lucas, R., Poitou, J., Nifenecker, H., Peter, J., Tamain, B.: Z. Physik A283, 257 (1977).

9. Kratz, J. V., Liljenzin, J. O., Norris, A. E., Seaborg, G. T.: Phys. Rev. C13, 2347 (1976).

10. Sikkeland, T.: Ark. Fys. 36, 539 (1966).

11. Moretto, L. G., Schmitt, R.: J. de Physique C5, 109 (1976).

12. Lefort, M.: J. de Physique C5, 57 (1976).

13. Otto, R. J., Seaborg, G. T., Fowler, M. M.: to be published in Phys. Rev. C (1978).

14. Myers, W. D.: Atomic Data and Nucl. Data Tables 17, 411 (1976).

15. Cohen, S., Plasil, F., Swiatecki, W. J.: Ann. Phys. 82, 557 (1974).

16. Northcliffe, L. C., Schilling, R. G.: Nucl. Data A7, 223 (1970).

17. Guttner, K., Hofmann, S., Marx, D., Muzenberg, G., Nickel, F.: Nucl. Inst. Meth. 146, 413 (1977).

18. Saint-Simon, M. de, Otto, R. J., Seaborg, G. T.: Lawrence Berkeley Laboratory Report LBL-7114 (1978), to be submitted to Phys. Rev. C.

19. Binder, I.: Ph.D. thesis, University of California, Berkeley, California, Lawrence Berkeley Laboratory Report LBL-6526 (1977).

Figure Captions

Fig. 1. Experimental (solid lines) and calculated (dashed lines) recoil range distributions for the reaction of 259 MeV $^{40}Ar + ^{197}Au$. The bottom axis indicates the position and number of each of the forward recoil foils (1-8), the Target (T) and the backward recoil foils (A,B).

Fig. 2. Experimental (solid line) and calculated (dashed line) recoil range distributions for ^{237}Pu and the combined products of Te, I, Xe, and Cs and of Hf, Ta, W, Re, and Os from the reaction 250 MeV $^{40}Ar + ^{238}U$. See Fig. 1 for an explanation of the axes.

Fig. 3(A) The experimental recoil range distributions for Hg(Tl) products from the three reactions, 276 MeV $^{48}Ca + ^{238}U$ and 239 and 250 MeV $^{40}Ar + ^{238}U$. The excitation energies, E*, for the compound nucleus system are also given. (B) The calculated recoil range distributions for the same reactions as shown in (A). The three calculated distributions shown in (B) for each of the Hg(Tl) distributions were calculated using the angular distributions in (C) denoted by the same type of line.

Table I. Summary of experiments.

Projectile	Target[a]	E_{lab}[c] (MeV)	Compound Nucleus (CN)	E^*_{CN} (MeV)[d]
^{48}Ca	^{238}U	276 ± 8	$(^{286}112)$	64
^{40}Ar	^{238}U	237 ± 7	$(^{278}110)$	68
^{40}Ar	^{238}U	250 ± 8	$(^{278}110)$	79
^{40}Ar	^{243}Am[b]	214-300	$(^{283}113)$	39-113
^{40}Ar	^{197}Au	259 ± 8	$(^{237}_{97}Bk)$	98

[a] The uranium target consisted of 0.5 to 1.0 mg/cm^2 UF_4 on 3.43 mg/cm^2 aluminum backing. The gold target was 2.4 mg/cm^2 gold foil.

[b] Experiments reported in Ref. 4.

[c] Beam energy at the center of the target.

[d] Calculated from the mass table of Myers and Swiatecki (private communication), and Ref. 14.

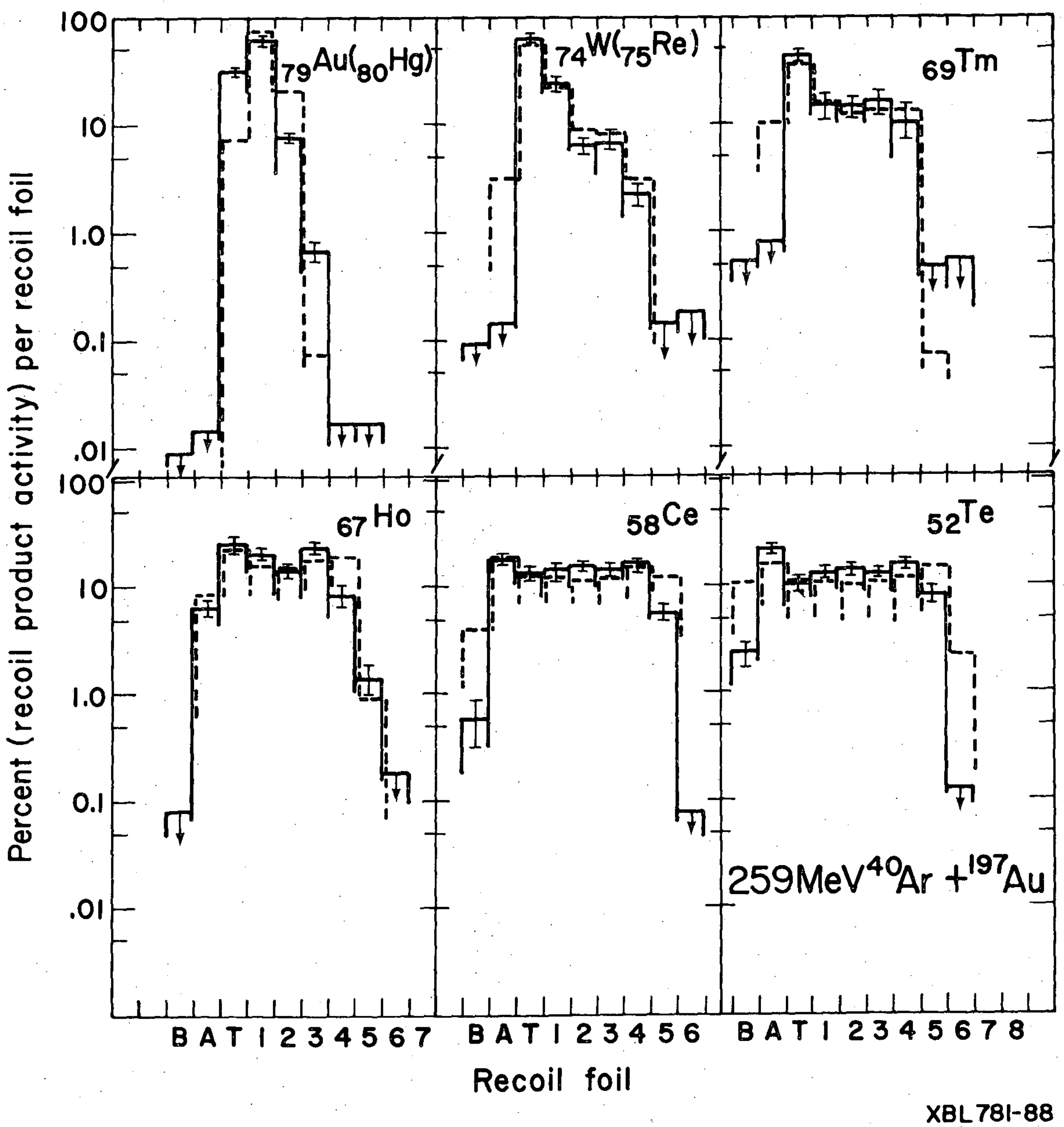
100
10
1.0
0.1
.01
$_{79}$Au($_{80}$Hg)
$_{74}$W($_{75}$Re)
$_{69}$Tm
$_{67}$Ho
$_{58}$Ce
$_{52}$Te
Percent (recoil product activity) per recoil foil
B A T 1 2 3 4 5 6 7
B A T 1 2 3 4 5 6
B A T 1 2 3 4 5 6 7 8
Recoil foil
259MeV ^{40}Ar + ^{197}Au
XBL781-88

Fig. 1

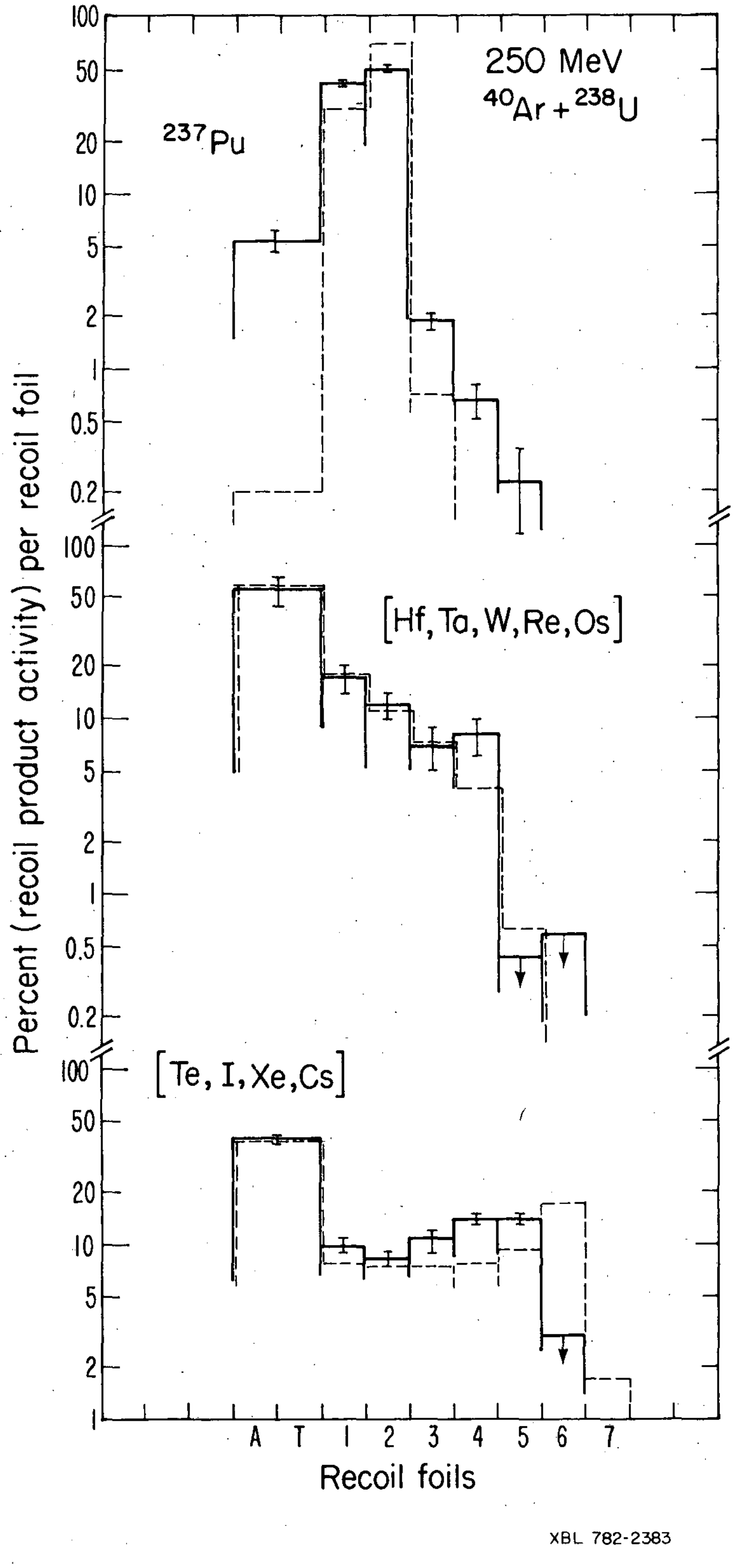

100
50
20
10
5
2
1
0.5
0.2
250 MeV
$^{40}Ar + ^{238}U$
^{237}Pu
[Hf, Ta, W, Re, Os]
[Te, I, Xe, Cs]
Percent (recoil product activity) per recoil foil
A T 1 2 3 4 5 6 7
Recoil foils
XBL 782-2383

Fig. 2

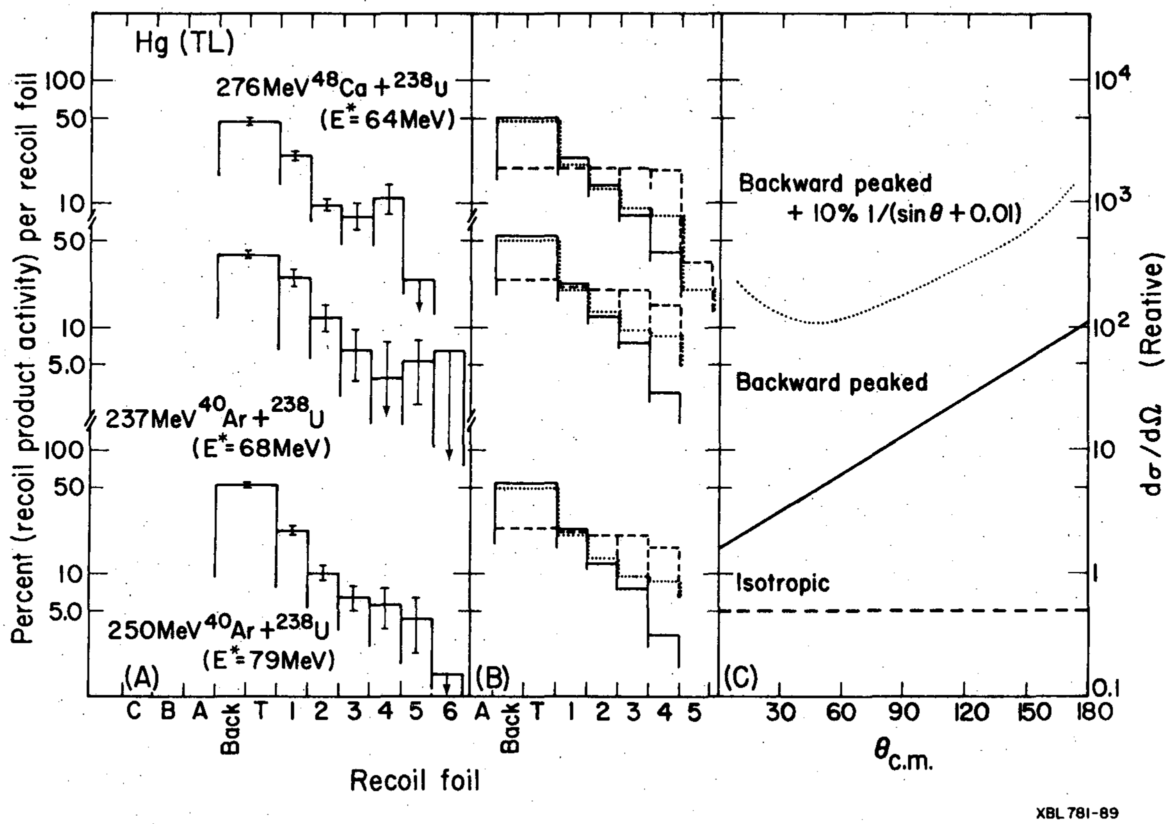

Hg (TL)
276MeV ^{48}Ca + ^{238}U
(E* = 64MeV)
237MeV ^{40}Ar + ^{238}U
(E* = 68MeV)
250MeV ^{40}Ar + ^{238}U
(E* = 79MeV)
Percent (recoil product activity) per recoil foil
(A)
(B)
(C)
C B A Back T 1 2 3 4 5 6 A Back T 1 2 3 4 5
Recoil foil
Backward peaked + 10% 1/(sin θ + 0.01)
Backward peaked
Isotropic
dσ/dΩ (Relative)
30 60 90 120 150 180
θc.m.
XBL 781-89

Fig. 3

This report was done with support from the Department of Energy. Any conclusions or opinions expressed in this report represent solely those of the author(s) and not necessarily those of The Regents of the University of California, the Lawrence Berkeley Laboratory or the Department of Energy.

TECHNICAL INFORMATION DEPARTMENT
LAWRENCE BERKELEY LABORATORY
UNIVERSITY OF CALIFORNIA
BERKELEY, CALIFORNIA 94720